BMC Genomics

RESEARCH Open Access

Oysters in transition: hermaphrodite oysters display unique DNA methylation patterns in gill tissue

Sophie Valk[1], Marc Engelsma[2], Hendrik-Jan Megens[3], Pauline Kamermans[1,4], Albertinka J. Murk[1] and Reindert Nijland[1*]

Abstract

Background European flat oysters (*Ostrea edulis*) are sequential hermaphrodites that alternate sex in response to environmental change. Epigenetics, including DNA methylation, are often involved in sex reversal through influencing gene transcription. Knowledge on the epigenetic mechanisms underlying sex reversal in hermaphrodite bivalves is limited to gonadal tissue and previous studies have only compared DNA methylomes of males and females. Therefore, the aim of this study is to assess whether sex-specific DNA methylation can be identified in somatic gill tissue of the flat oyster.

Results By comparing whole-genome methylomes of 35 oysters of different sex phenotypes using nanopore sequencing, we demonstrate the presence of sex-specific DNA methylation patterns in somatic gill tissue. A total of 9,654 regions and 2,576 genes were differentially methylated between male, female, and hermaphrodite oysters. Functional analysis of differentially methylated genes indicated an association with energy homeostasis and metabolic processes, implying a remodeling of the energy balance.

Conclusions This study is the first to characterize DNA methylomes of hermaphrodite oysters, providing new insights into the epigenetic mechanisms underlying sex reversal in a sequential hermaphrodite invertebrate. Additionally, this study characterizes sex-specific DNA methylation in somatic gill tissue, paving the way for non-lethal sex identification using epigenetic biomarkers.

Keywords DNA methylation, Epigenetics, European flat oyster, Gill tissue, Sex differentiation, *Ostrea edulis*, Sequential hermaphrodite

Introduction

Epigenetic mechanisms influence gene transcription without changing the DNA sequence itself [1]. DNA methylation, the covalent transfer a methyl group to a DNA nucleotide, is one of the most common epigenetic modifications in eukaryotes and is involved with various developmental and regulatory processes [2, 3]. In vertebrates, DNA methylation occurs primarily on CpG islands where de-methylation often results in gene silencing [4, 5]. Contrasting to vertebrates, invertebrates acquire a more mosaic pattern of DNA methylation, mainly occurring on gene bodies [6, 7]. Reduced gene

*Correspondence:
Reindert Nijland
Reindert.nijland@wur.nl
[1] Marine Animal Ecology, Wageningen University and Research, Wageningen 6700 AH, the Netherlands
[2] Wageningen Bioveterinary Research, Wageningen University and Research, Lelystad 8200 AB, the Netherlands
[3] Animal Breeding and Genomics, Wageningen University and Research, Wageningen 6700 AH, the Netherlands
[4] Wageningen Marine Research, Wageningen University and Research, Yerseke 4400 AB, the Netherlands

body methylation has the potential to facilitate transcriptional opportunities by alternative splicing, for example through exon skipping or by providing access to alternative transcription start sites [7, 8]. Growth, development, and environmental conditions can initiate de novo DNA methylation or change its maintenance [4, 9]. By influencing gene transcription, DNA methylation forms the crucial ingredient in facilitating phenotypic plasticity, whereby organisms can change their phenotype in response to changing environments [8]. Understanding the epigenetic mechanisms that are at the core of the interplay between the environment and phenotypic plasticity is pivotal for understanding how species respond to or cope with environmental change.

One prevalent example of phenotypic plasticity is sex reversal, by which an animal is capable of changing its phenotypic sex without the need for a corroborative change in DNA. Sex reversal occurs in many lineages of the animal kingdom, such as in reptiles [10], amphibians [11], fish [12], and a wide variety of invertebrates [13–17]. The plasticity and frequency with which animals can reverse sex are partly determined by the underlying sex determination mechanisms, which can be roughly divided into genetic sex determination (GSD) and environmental sex determination (ESD). The ability to reverse sex can be advantageous in highly dynamic environments, where sex-related differences in fitness may favour transition into one sex under specific environmental conditions [18–21]. During sex reversal, epigenetic mechanisms play a pivotal role in facilitating sex differentiation by influencing gene expression [8, 22–24].

Oysters represent excellent candidates for studying epigenetic mechanisms underlying sex reversal since they are sequential hermaphrodites that can repeatedly alternate between male and female sex phenotypes [15, 25, 26]. A variety of environmental factors have been documented to initiate sex reversal in oysters by altering DNA methylation (e.g. acidification [27] and starvation [28]), in the gonads. Differential DNA methylation between phenotypic sexes, referred to as sex-specific DNA methylation, are suggested to lead to sex differentiation by influencing gene transcription [14, 28–31]. Generally, energetically demanding or restricting conditions lead to masculinization of gonadal tissue [28, 32]. The association between DNA methylation and sex reversal has been primarily studied in gonad tissue, where sex-specific DNA methylation and gene expression are expected to have a direct relation to gametogenesis [33, 31]. In the Pacific oyster (*Magallana gigas*), differential methylation and expression of several genes are shown to be involved with sex differentiation in the gonads [29–31, 34]. Interestingly, during the process of sex reversal, oysters often display intermediate sex stages where they simultaneously produce male and female reproductive tissue of different developmental stages [15]. These individuals are characterized as hermaphrodites that display either male or female biased gonad tissue, or represent gonadal tissue containing both sexes with equal ratios [15, 35]. The simultaneous occurrence of male, female, and hermaphrodite individuals within one population is suggested to represent a phenotypically plastic response to temporally dynamic environments [36]. Although sequential hermaphroditism is frequently observed in oysters and hermaphrodite individuals contribute largely to reproductive cohorts in wild populations [36], previous studies have been exclusively comparing sex-specific DNA methylation between males and females [29, 30, 37]. Hence, sex-specific DNA methylation of hermaphrodite individuals remains poorly understood [15, 30, 36–38]. However, understanding how DNA methylation may differ between male, female, and hermaphrodite individuals is crucial for understanding the role of DNA methylation during different stages of sex reversal in oysters [38].

Currently, sex reversal in oysters is understudied, since existing methods of sex-identification require sampling of gonad tissue and are therefore lethal. Notably, sex-specific DNA methylation is not restricted to gonadal tissue and accommodates sex-associated differences in somatic tissues (e.g. mantle and abductor muscle) and even whole-body methylomes of different invertebrates [14, 39, 40]. This highlights the relevance of characterizing differential DNA methylation in somatic tissues between different sex phenotypes in oysters [14]. Gill tissue, along with other somatic tissues, is often collected during biosecurity or monitoring surveys where the tissue can be sampled non-lethally, by using anaesthetics [41, 42]. As such, identifying sex-specific methylation in somatic tissue would pave the way for non-lethal alternatives of sex-identification.

Like many other bivalves, the European flat oyster (*Ostrea edulis;* Linnaeus, 1758) is a sequential hermaphrodite that can reverse sex within one reproductive season [15, 25]. It plays a critical role in the ecosystem by sustaining biodiversity through generating biogenic reef habitats [43–45]. The species is currently considered 'threatened' according to the Oslo-Paris Convention, due to ongoing habitat degradation, overfishing, and the spread of diseases [46–49]. Recently, its decline in population stocks initiated restoration efforts to restock degraded populations with hatchery-produced oysters [44, 50, 51]. However, male-biased skewed sex ratios limit reproductive output and are thought to hamper the upscaling of oyster culturing used for kick-starting oyster reef restoration [35, 52]. Identifying epigenetic mechanisms that underly sex reversal is crucial for a better

understanding of the reproductive strategy of *O. edulis* and can facilitate in improving culturing strategies of the species [32, 38].

Therefore, this study aimed to assess whether sex-specific DNA methylation is present in somatic gill tissue, and to characterize the regional differences in sex-specific DNA methylation between male, female, and hermaphrodite flat oysters (*O. edulis*). By comparing gill methylomes using nanopore sequencing we show the presence of regional sex-specific DNA methylation across the genome. This study is the first to include DNA methylation of hermaphrodite individuals, providing new insights into the epigenetic mechanisms underlying sex reversal in a sequential hermaphrodite invertebrate. Additionally, this study highlights the potential of using somatic tissues to study sex reversal for non-lethal applications.

Results

Whole genome DNA methylomes obtained from gill tissue of flat oysters were compared between male, female, and hermaphrodite sex stages, with the aim of characterizing sex-specific DNA methylation. Oyster sex was identified using histology and five sex stages were distinguished: male (M), female (F), hermaphrodite predominantly male (HPM), hermaphrodite predominantly female (HPF), and hermaphrodite both sexes equally present (HBS). In total, whole-genome sequencing of 35 flat oyster individuals resulted in 111 million reads, with an average of 3.2 million reads per individual (Supplementary Table S1). Sequencing of all oysters was performed on 8 different 10.4 PromethION flow cells. Mapping of reads with minimal quality of 60 to the *O. edulis* reference genome (XbOstEdul1.1), resulted in an average of 12.2 Gb per individual with read lengths varying between 1.1 −14.6 Kb and an average mapping percentage of 86.9% (Supplemental Table S1; submitted to ENA under accession number PRJEB85091). No significant difference in number of sequenced base pairs was observed between the five sex phenotypes (one-way ANOVA, F statistic = 0.872, *p*-value = 0.49; Supplementary Fig S1A). After CpG calling using *modkit*, between 10.4 and 30.5 million CpGs per individual, with a minimum coverage of 3, were used for downstream analysis.

General methylation patterns

Analysis of differentially methylated loci (DML) resulted in 555,259 CpG loci that were differentially methylated between any of the five sex phenotypes, with minimal coverage of 3 for all individuals. These CpGs were used as input for PCA analysis representing all sites that were differentially methylated between any two of the five sex phenotypes (Fig. 1A). PC1 (13.1% variance explained) shows clear separation between the five sex phenotypes with a gradient from male and female, to the three hermaphrodite sex phenotypes (HPM, HPF, and HBS).

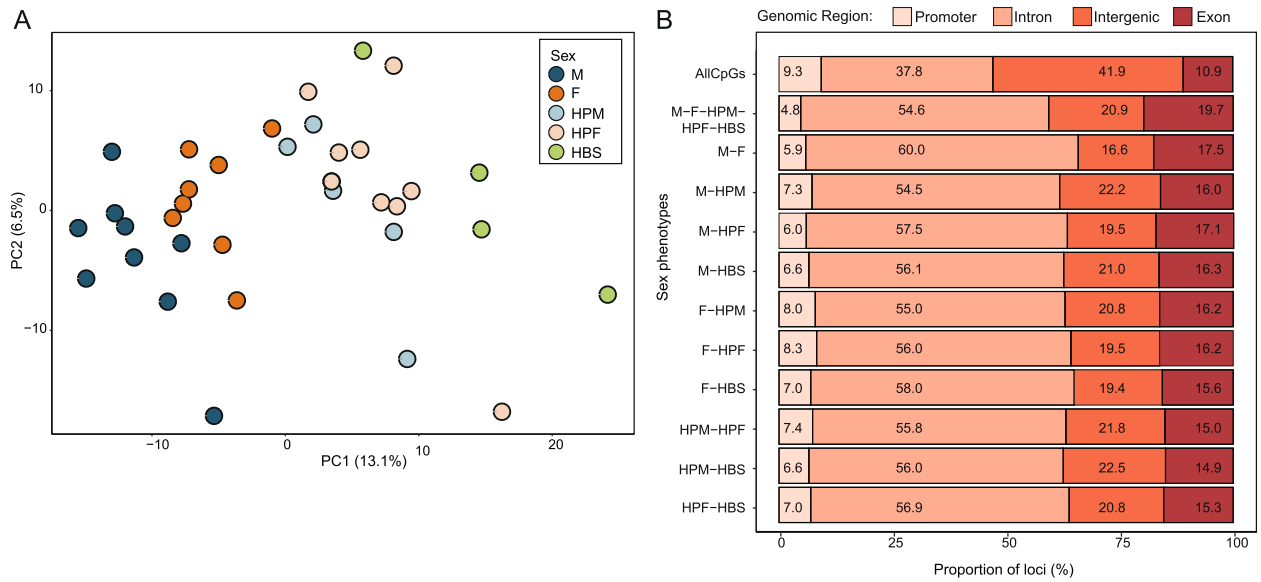

Fig. 1 Comparative analysis of differentially methylated loci (DMLs) between five sex phenotypes of flat oysters (M, F, HPM, HPF, and HBS). **A** Principal component analysis of all differentially methylated CpGs between any two of the five sex phenotypes (555,259 sites). **B** Distribution over genomic location of CpGs (minimal coverage of 3), DMLs identified from comparisons between any two of the five sex phenotypes, and DMLs from pairwise comparisons between the five sex phenotypes

Differentially methylated loci and regions between sex phenotypes

Characterization of DMLs between all five sex stages resulted in a total of 1506 loci in which minimally two sex phenotypes showed significant differential methylation (BH corrected q-value < 0.01, ≥ 20% methylation difference; Supplementary Table S2). The pairwise comparison between HPM and HBS resulted in the highest number of DMLs (27,363 DMLs; 13,366 hypermethylated in HBS, and 13,997 hypermethylated in HPM; Supplementary Fig. S2A). Between M-HPF 4136 DMLs were identified, representing the lowest number of DMLs from all pairwise comparisons, followed by 4252 DMLs between F-HPF (Supplementary Fig. S2A).

The majority of DMLs were located in introns (56.6%), followed by intergenic regions (20.4%), exons (16.0%), and promoters (7.0%; Fig. 1B). The genomic distribution of significant DMLs from pairwise comparisons between sex phenotypes differed significantly from the genomic distribution of all CpGs (minimal coverage of 3 for all individuals; Pearson's correlation: p-value < 0.05; Supplementary Table S3). Here, significant DMLs found between pairwise comparisons showed a positive association with intronic regions, and a negative association with intergenic regions.

Characterization of differentially methylated regions (DMRs) using a sliding-window approach resulted in a total of 21,160 significant DMRs from pairwise comparisons between any two of the five sex phenotypes (BH corrected q< 0.01, ≥ 20% methylation difference; Supplementary Table S4). Merging DMRs that were within 100 bp proximity of each other obtained a total of 9,651 DMRs that varied in length of 201 to 4001 base pairs (Supplementary Table S4). Generally, hermaphrodite sex phenotypes HPM and HBS showed higher numbers of DMRs than pairwise comparisons with or among males, females, or HPF. The highest number of DMRs was found between HPM and HBS (3369 DMRs, 1829 hypermethylated in HPM, and 1540 hypermethylated in HBS; Supplementary Fig. S2B). The lowest number of DMRs weas observed between females and HPF (164 DMRs; 84 hypermethylated in females, and 80 hypermethylated in HPF). Methylome comparison between males and females resulted in a total of 239 DMRs (125 hypermethylated in males, 114 hypermethylated in females). Two examples of DMRs between sex phenotypes have been visualized (Fig. 2A,B).

Gene annotation of differential methylation

Identifying differentially methylated genes (DMGs), genes overlapping with DMRs, resulted in a total of 2,576 unique DMGs between pairwise comparisons of all five sex phenotypes (Fig. 2C). Of all these genes, 828 unique DMGs were identified between HPM and HBS. Males, HPM, and HBS showed to have the highest overlap in DMGs (Fig. 2). Clustering analysis also revealed highest similarity in DMGs between M-HBS, and HPM-HBS. Additionally, F-HPM, M-HPM, and HPM-HPF also showed high similarity in identified DMGs, but clustered as a separate group with unique DMGs (Fig. 2D). The DMGs with highest difference in average methylation percentage between pairwise comparisons were: *MAM and LDL-receptor class A domain-containing protein 2-like* (LOC125683627; HPM-HBS), *UDP-GalNAc:beta-1,3-N-acetylgalactosaminyltransferase 2-like* (LOC125659768; F-HPM and F-HPM), *ATP-dependent DNA helicase Q5-like* (LOC125679612; M-HBS), and *sacsin-like* (LOC125679280; HPM-HBS; Table 1). A complete overview of the top 10 most hypermethylated and hypomethylated DMGs identified for all pairwise comparisons can be found in the supplementary material (Supplementary Table S5).

In total, 125 genes were found to be differentially methylated between male and female oysters, of which 62 DMGs were hypermethylated in males, and 63 DMGs were hypermethylated in females (Supplementary Table S6). When compared to DMGs identified between other sex phenotypes, 15 DMGs were uniquely differentially methylated between males and females (Supplementary Table S6). DMGs with highest difference in methylation percentage between males and females were: *tRNA (guanine-N(7)-)-methyltransferase non-catalytic subunit wdr4-like (*LOC125645763), uncharacterized LOC125655458, uncharacterized LOC125673983, where males were hypermethylated compared to females. DMGs with highest difference in average methylation percentage and females showing hypermethylation compared to males were: uncharacterized LOC125661226,

(See figure on next page.)

Fig. 2 Differentially methylated regions (DMRs) and genes (DMGs) from gill methylome comparisons between five sex phenotypes (M, F, HPM, HPF, and HBS) in flat oysters. **A** DNA methylation profile of all 35 flat oyster individuals at the position of gene LOC125645858. Vertical bars represent methylation percentages per CpG site from 0–100%. Black boxes indicate DMR areas. **B** DNA methylation profile of all male and female oyster individuals at the position of gene LOC125647918. Vertical bars represent methylation percentages per CpG site from 0–100%. **C** Upset plot showing the number of overlapping and unique DMGs (n = 2,576) identified from pairwise comparisons between the five sex. **D** Hierarchical clustering of overlap in DMGs (n = 2,576) between the five sex phenotypes using Pearson's correlation coefficient

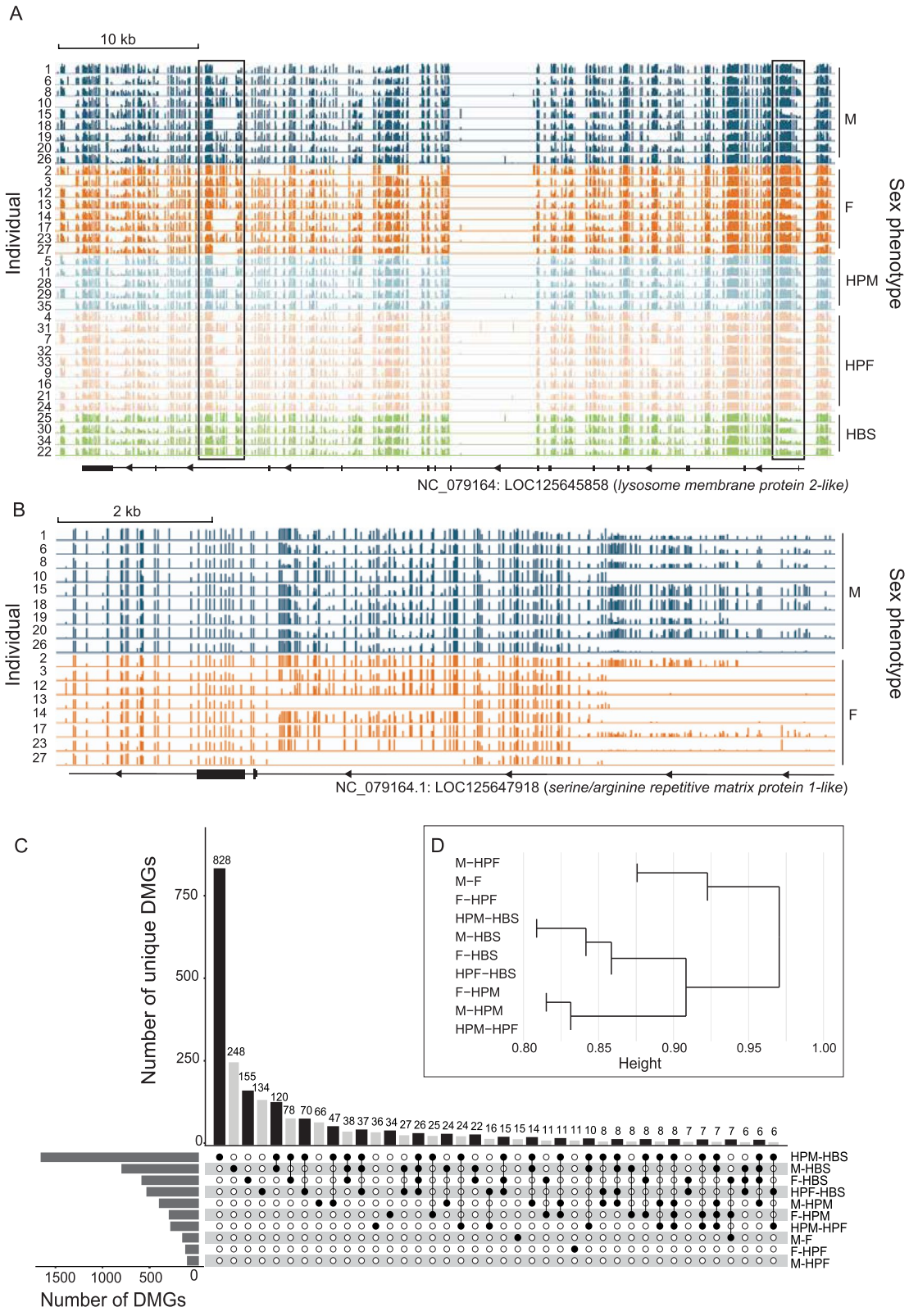

Fig. 2 (See legend on previous page.)

Table 1 Overview of the top most hypermethylated and hypomethylated DMGs for pairwise comparisons between all five sex phenotypes (M, F, HPM, HPF, and HBS)

Gene ID	Gene Description	Pairwise Comparison	Pseudochromosome	Length	Methylation (%)	Adjusted qvalue
LOC125652448	transport and Golgi organization protein 6 homolog	M-F	NC_079164.1	1301	-53.3680433178866	2.96208951245896E-052
LOC130051844	ester hydrolase C11orf54 homolog	M-F	NC_079164.1	301	37.2582417582418	1.61137197226376E-021
LOC125645560	proton-coupled zinc antiporter SLC30 A2-like	M-HPM	NC_079169.1	1701	-54.8091058670907	8.10987876182568E-037
LOC130050362	uncharacterized LOC130050362	M-HPM	NC_079172.1	301	47.4035563592526	6.92625857610277E-037
LOC125652448	transport and Golgi organization protein 6 homolog	M-HPF	NC_079164.1	401	-42.175698181644	1.27453457293131E-046
LOC130051844	ester hydrolase C11orf54 homolog	M-HPF	NC_079164.1	301	37.2582417582418	1.61137197226376E-021
LOC125679612	ATP-dependent DNA helicase Q5-like	M-HBS	NC_079165.1	901	-60.2998006773845	8.6947215528774E-042
LOC125670462	protocadherin Fat 4-like	M-HBS	NC_079167.1	201	52.0976094204441	1.67199085281488E-031
LOC125659768	UDP-GalNAc:beta-1,3-N-acetylgalactosaminyltransferase 2-like	F-HPM	NC_079172.1	301	-50.8465939360249	6.72229257813295E-043
LOC125655710	uncharacterized LOC125655710	F-HPM	NC_079170.1	201	61.8869420254375	4.9771803906424E-070
LOC125675975	uncharacterized LOC125675975	F-HPF	NC_079166.1	301	-40.6276149185132	1.85859901577164E-033
LOC125658752	arsenite methyltransferase-like	F-HPF	NC_079172.1	201	40.3920477137177	7.05313397251047E-032
LOC125675975	uncharacterized LOC125675975	F-HBS	NC_079166.1	301	-50.5105617059029	1.61397292093311E-031
LOC125679490	putative polypeptide N-acetylgalactosaminyltransferase 10	F-HBS	NC_079165.1	201	51.5837104072398	8.53880056942331E-040
LOC125660846	ATP-binding cassette sub-family B member 6-like	HPM-HPF	NC_079171.1	301	-47.2298409261188	2.49588780513731E-018
LOC125659768	UDP-GalNAc:beta-1,3-N-acetylgalactosaminyltransferase 2-like	HPM-HPF	NC_079172.1	201	56.2110240874834	1.77573266151024E-055
LOC125679280	sacsin-like	HPM-HBS	NC_079165.1	1201	-62.4605706501535	1.14454321578361E-048
LOC125683627	MAM and LDL-receptor class A domain-containing protein 2-like	HPM-HBS	NC_079169.1	601	62.6613682616021	4.54624205126091E-032
LOC125681288	uncharacterized LOC125681288	HPF-HBS	NC_079164.1	201	-51.4323730742718	1.01037750392091E-039
LOC125673062	uncharacterized LOC125673062	HPF-HBS	NC_079166.1	201	49.1092278719397	1.14601071580134E-032

uncharacterized LOC125661253, and *periodic tryptophan protein 1 homolog* (LOC125674140). Other DMGs uniquely identified between male and female oysters were: *cyclic AMP-dependent transcription factor ATF-2-like* (LOC125646345), *inhibitor of nuclear factor kappa-B kinase subunit alpha-like* (LOC125668035), *neuronal calcium sensor 2-like* (LOC125669759), *PR domain zinc finger protein 4-like* (LOC125680421), and *zinc finger protein 474-like* (LOC130054705).

Functional enrichment analyses

Analysis of difference in average methylation percentage over all DMRs within a DMGs resulted in 21 DMGs with a difference in average methylation percentage > 45%. DMGs with highest difference in average methylation percentage were *proton-coupled zinc antiporter SLC30 A2-like* (LOC125645560; HPM-HBS), *MAM and LDL-receptor class A domain-containing protein 2-like* (LOC125683627; HPM-HBS), LOC125655710 (F-HPM), *and probable nuclear hormone receptor HR3* (LOC125661857; M-HPM & F-HPM), *ATP-dependent DNA helicase Q5-like* (LOC125679612; Me-HBS), and *protein ILRUN-like* (LOC125645979; M-HBS; Fig. 3B). Differential methylation between HPM-HBS was observed in the *lysosome membrane protein 2-like gene* (LOC125645858), belonging to the superfamily of ABC transporters [53].

Functional enrichment analysis of Gene Ontology (GO) terms of annotated DMGs resulted in 128 significant enriched GO terms for Biological Processes (BP; Fig. 3A), 45 enriched GO terms for Cellular Components (CC; Supplementary Figure S4), and 64

(See figure on next page.)

Fig. 3 Functional annotation of differentially methylated genes (DMGs) identified from pairwise comparisons of the five sex phenotypes (M, F, HPM, HPF, and HBS). **A** Heatmap of Gene Ontology (GO) of DMGs ($n = 2,576$) enriched for Biological Processes (BP; $n = 128$). BP were clustered hierarchically with Pearson's correlation coefficient. **B** Heatmap of DMGs with an average difference in methylation percentage > 45%. Positive differences in average methylation percentage indicate hypomethylation for the first group per pairwise comparison, negative differences in average methylation percentage indicate hypermethylation for the first group per pairwise comparison. **C** Scatter plot of enriched Kyoto Encyclopedia of Genes and Genomes (KEGG) pathways for DMGs identified between the five sex phenotypes

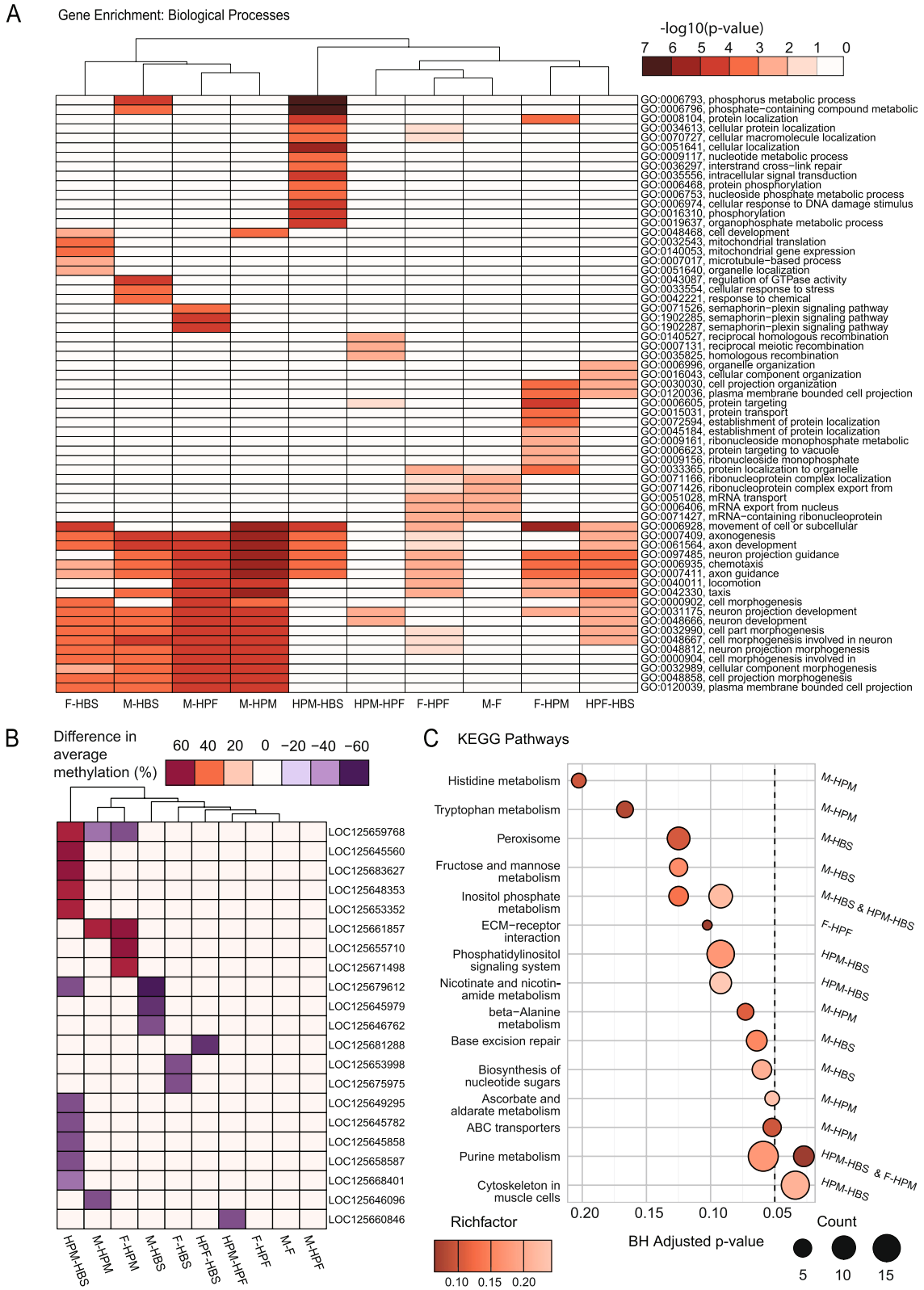

Fig. 3 (See legend on previous page.)

enriched GO terms for Molecular Function (MF; Supplementary Figure S5). GO terms for Biological Processes were related to neuronal activity and locomotion (e.g. GO0061564: axon development, GO0048666: neuron development, GO0040011: locomotion, and GO0006935: chemotaxis), protein targeting and localization (e.g. GO0006605: protein targeting and GO0015031: protein transport) and cellular and metabolic processes (e.g. GO0030030: cell projection organization, GO0051641: cellular localization, GO0009117: nucleotide metabolic process, and GOGO0006793: phosphorus metabolic process). Processes related to stress response were enriched in DMGs found between males and HBS (GO0043087: regulation of GTPase activity, GO0033554: cellular response to stress, and GO0042221: response to chemical").Additionally, DMGs found between males and HPF were enriched in the "semaphorin-plexin signalling pathway" (GO0071526, GO1902285, GO1902287). Lastly, unique GO terms found between HPM-HPF were related to meiotic recombination (GO0140527, GO0007131, and GO0035825).

Regarding CC, the largest group of DMGs showed enrichment for "intracellular anatomical structure" (GO0005622) and "organelle" (GO0043226; Supplementary Figure S3. DMGs enriched in MF were mostly related to pathways associated with nucleotide binding (e.g. GO0005488: binding, GO0005524: ATP binding, GO0030554: adenyl nucleotide binding, and GO0032559: adenyl ribonucleotide binding"; Supplementary Figure S4). Here, DMGs identified between HPM and HBS contributed mostly to these enriched pathways.

Kyoto Encyclopedia of Genes and Genomes (KEGG) analysis of DMGs revealed 25 enriched pathways, of which 2 significant ($p_{adjust} < 0.05$; Fig. 3C). The most significantly enriched pathways were involved in "Cytoskeleton in muscle cells" and "purine metabolism". Enriched pathways were mostly related to energy homeostasis due to their association with lipid, amino acid, and carbohydrate metabolism (e.g. "Purine metabolism", "Ascorbate and aldarate metabolism", "Beta-Alanine metabolism", "Inositol phosphate metabolism", and "Nicotinate and nicotinamide metabolism"). In addition to metabolism related pathways, DMGs from pairwise comparisons also showed enrichment for processes related to innate immunity (e.g. "ABC transporter" and "Peroxisome"; Fig. 3C).

Discussion

In invertebrates, DNA methylation is thought to contribute to phenotypic plasticity by increasing transcriptional variation in various ways (e.g. alternative splicing, increasing mutation rate) [8]. The mosaic gene-body methylation is suggested to create transcriptional opportunities rather than activate or inhibit transcription through (de)methylation in the promoter region [8]. Sex reversal, a phenotypically plastic trait whereby animals can reverse sex in response to environmental change, is associated with DNA methylation where differences between sexes are thought to facilitate this reversal [11, 22, 29, 54–57]. Sex-specific DNA methylation has been widely reported in both vertebrates and invertebrates [22, 58–62]. In oysters, differential DNA methylation between male and female individuals is suggested to be associated with sex differentiation in the gonads, where epigenetic differences are linked to differential expression of genes involved in the sex determination pathway [28–30]. Although oysters are sequential hermaphrodites, knowledge on DNA methylation profiles of hermaphrodite individuals, undergoing a sex change, is limited. In this study, we aimed to characterize sex-specific DNA methylation of male, female and hermaphrodite European flat oysters (*Ostrea edulis),* by comparing gill methylomes obtained through nanopore sequencing. In general, differential methylation occurred more frequently in intragenic regions (promoters, introns, and exons) than in intergenic regions. These findings are consistent with results from other oyster species, where differential methylation is enriched in intergenic regions [63–65]. The most distinct DNA methylation profile was observed in hermaphrodite oysters, whereas males and females demonstrated more similar patterns of DNA methylation in their gills. Functional enrichment analysis indicated that differentially methylated genes (DMGs) were significantly enriched in pathways related to energy homeostasis and metabolism. Collectively, our data suggests that sequential hermaphrodites display an alternative state that represents the epigenetic reprogramming required for sex reversal. Additionally, the observed presence of sex-specific DNA methylation in gill tissue highlights the potential for non-lethal sex identification using somatic tissues.

Hermaphrodite individuals display an alternative epigenetic state in the gills

When oysters undergo sex reversal, gametogenesis of both sexes can occur within the same follicle [15]. In these hermaphrodites, discrepancies in gamete development most often lead to asynchronous spawning of male and female gametes [15]. In the gonads, the reversal of sex is accompanied by epigenetic reprogramming that facilitates cell growth, development, regulation, and restructuring, especially during early gametogenesis [30, 66]. In this study, whole-genome gill methylome

comparisons between sex phenotypes demonstrated that hermaphrodites display the most distinct DNA methylation patterns when compared to males or females. Significantly enriched GO terms overlapping DMGs found between hermaphrodites and other sex phenotypes were related to neuronal activity and locomotion, and cell morphogenesis pathways. Additionally, the KEGG pathway related to "Cytoskeleton in muscle cells" was significantly enriched between hermaphrodite oysters. These findings suggest that hermaphrodite individuals undergoing sex reversal display an alternative state of epigenetic reprogramming when compared to males or females. It is possible that males and females, that have undergone the full process of sex reversal, represent an epigenetic state that matches the completion of sex reversal. Similarly, in a study of Sun et al. (2024), genome-wide DNA methylation patterns of gonadal tissue of *Magallana gigas* were accurately remodeled to the opposite sex after the completion of sex reversal [30].

In addition to the differential methylation patterns observed between male, female, and hermaphrodite individuals, numerous unique GO terms were identified between the different hermaphrodite sex phenotypes (HPM, HPF, and HBS). The majority of differentially methylated loci and regions (DMLs and DMRs) were identified between HPM and HBS. DMGs overlapping those regions showed significant enrichment for processes related to "cellular localization", "intracellular signal transduction", "phosphorylation" and "phosphate metabolism". The differences in annotated GO terms identified across hermaphrodite sex phenotypes imply that the direction of sex reversal is also associated with differential DNA methylation. In *M. gigas*, a genome-wide increase in DNA methylation was observed when oysters reversed sex from female to male [30]. While further elucidation of epigenetic reprogramming in hermaphrodite phenotypes is necessary to validate this, the highest number of DMLs and DMRs found between HPM-HBS suggests that the direction of sex reversal is associated with different epigenetic states. This supports the hypothesis that although sex reversal is bidirectional, patterns of epigenetic reprogramming may be different depending on the direction of a sex reversal event.

Sex-specific DNA methylation of gill tissue is related to energy homeostasis and metabolism

In this study, functional enrichment analysis of DMGs resulted in highest significant enrichment for GO-terms related to metabolic or energy homeostasis processes (e.g. ATP binding, nucleotide binding, hydrolase activity, DNA damage sensor activity). Similar to our findings, differential methylation and expression between prespawning and postspawning oysters was enriched for metabolism and energy homeostasis pathways in gill tissue of *M. gigas* [67]. KEGG enrichment analysis of DMGs resulted in enriched pathways related to lipid, amino-acid, and carbohydrate metabolisms (e.g. "purine metabolism", "ascorbate and aldarate metabolism", "beta-Alanine metabolism", "nicotinate and nicotinamide metabolism"). The purine metabolism plays an essential role in energy supply, where it is involved in synthesis, degradation, and recycling of nucleic acids [68]. In the mussel *Mytilus coruscus,* a reduction in energy consumption in the gills was observed after starvation exposure, where proteins related to purine metabolism and nicotinic and nicotinamide metabolism pathways were downregulated [68]. Additionally, the inositol phosphate metabolism pathway, enriched in DMGs identified between M-HSB and HPM-HBS, contributes to metabolic signaling, and cellular reprogramming and growth in oysters [69, 70]. Similarly, GO terms related to innate immunity, cell proliferation, and metabolic and developmental processes were enriched in transitionary transcripts of sex reversing wrasses [23]. Gametogenesis requires excessive amounts of energy due to enhanced cell growth, cellular restructuring, and reprogramming [71, 72]. Therefore, it is likely that oysters undergoing sex reversal require a remodeling of the energy balance in all their tissues, reflecting processes of cell restructuring and rebuilding. The sex-specific differences in genes related to energy homeostasis and metabolism observed in this study, could be explained by a remodeling of the energy balance due to changes in energy requirement as a consequence of sex reversal.

Changes in immunity and stress response as a consequence of sex-specific DNA methylation

In addition to changes in DNA methylation of genes related to energy homeostasis and metabolism, DMGs found between the different sex phenotypes were also enriched in pathways related to immunity, stress, and toxin response. ATP-binding cassette (ABC) transporters play a key role in the defensive mechanism against pathogens in bivalves [73, 74]. Furthermore, peroxisomes are crucial in toxin response mechanisms [75]. Lysosome membrane proteins are involved in the cellular defensive response and vital for the production of phagolysosomes [76]. Phagocytosis can have multiple functions in bivalves, namely enhanced innate immune response, or energy recycling by the reabsorption of damaged cells, which can be initiated by sex reversal [77]. Upregulation of the phagocytosis pathway was observed in gill proteomes after starvation exposure in the mussel *M. coruscus* [68]. One probable explanation of the observed differences in DNA methylation is that oysters of different sex phenotypes adopt different metabolic and

immune response strategies depending on their energy requirements for reproduction. Notably, gametogenesis can lead to enhanced susceptibility to pathogens due to increased energetic demands required for reproduction [78]. During gametogenesis, reduced phagocytosis activity of hemocytes has also been reported in oysters [79]. Similarly, immunity and stress response pathways were found to be enriched in differentially expressed genes identified between pre- and postspawning oysters [67]. Postspawning oysters are reported to experience a decrease in global immunity defense and become more vulnerable to chemical stress, due to energy loss after spawning [67, 80]. However, this study only assessed the differences in sex-specific DNA methylation, therefore, statements on how sex-specific DNA methylation in gill tissue affects functionality of these genes remains speculative and should be interpreted with caution.

Somatic sexual dimorphism as a consequence of DNA methylation differences between male and female oysters

Although comparison of DNA methylation between male and female oysters yielded the lowest number of DMRs and DMGs, 125 DMGs could still be identified of which 15 were uniquely differentially methylated between males and females. Most of these unique DMGs were related to metabolic, signaling, or expression related processes. Guanine-N7-methyltransferases are involved in modifications of mRNA caps and required for mRNA processing and functioning [81]. Cyclic adenosine monophosphate (cAMP) activity is involved in regulating glycogen breakdown, and suggested to be related to the control of gonad maturation [82]. Another unique DMG found between male and female oysters was *inhibitor of nuclear factor kappa-B kinase (*IKK*) subunit alpha-like.* IKKs play a central role in cell signalling and are involved with innate immunity in oysters [83]. Besides the unique DMGs identified between males and females, other DMGs with high difference in methylation percentage between male and female oysters are associated with pathways that regulate somatic sexual dimorphism in other animals. For example, the serine/arginine repetitive matrix protein (SRRM) was observed to be expressed in the gonads and has been allocated as a candidate sex-identification marker in a shrimp species [84]. In *Drosophila melanogaster,* SRRM1 is involved in genitalia development and somatic sex determination [85, 86]. Additionally, *Transport and Golgi organization protein 6 homolog* (TANGO6) is associated with mating behaviour in seahorses, where differential expression in somatic brain tissue was observed during mating [87]. In zebrafish, sex-specific DNA methylation was observed in genes associated with the arsenic metabolism, which was suggested to lead to sex-specific behavioural changes [88]. Likewise, the arsenic metabolism appears to be gender-specific in rats [89]. Another interesting gene that was differentially methylated between males and females was prostaglandin E synthase 3-like. Prostaglandins are involved with ovary development and steroidogenesis in other bivalves [90]. DMGs related to the semaphorin-plexin signaling pathway were solely enriched between M and HPF. Semaphorin proteins are involved in immune system regulation and are crucial for nervous system development [91]. Additionally, semaphorin proteins were discovered to be involved in the development of neurons that secrete gonadotropin-releasing hormones in vertebrates, which are essential for reproductive development [91]. The ECM-receptor interaction pathway was solely enriched between F-HPF. Extracellular matrix (ECM)-receptor interactions were shown to be enriched in skin transcriptomes of female fish compared to males upon exposure to sex steroids [92]. Lastly, *MAM and LDL-receptor class A domain-containing protein 2-like* are involved in ovarian development in clams [90]. These examples indicate that even though sex reversal mostly impacts gonadal tissue, somatic tissues are not left unchanged and sex reversal can induce sex-specific processes of cell restructuring or reprogramming in somatic tissues accordingly. Sexual dimorphism is not as profound in oysters as in some other animals, however, indicators of sexual dimorphism are present (e.g. differences in growth or innate immunity [67]). Based on the findings of this study, we hypothesize that differential DNA methylation between male and female oysters is associated with sexual dimorphism in somatic tissues as a consequence of sex reversal. However, understanding the link between sex-specific DNA methylation and sexual dimorphism requires further elucidation of the effects of sex-specific DNA methylation on gene functioning.

Tissue specificity of sex-specific DNA methylation in oyster gills

The occurrence of sex-specific DNA methylation has been reported in various animals and tissue types [14, 61, 93–95]. However, literature is inconsistent on the existence of tissue specificity for sex-specific DNA methylation as some studies clearly show altered sex-specific DNA methylation in different tissue types [14, 29], whereas other studies demonstrate consistent sex-specific whole-body methylomes [93, 96]. In a study of Teng et al. (2025), similar DMGs were identified in somatic muscle and gonadal tissue between male and female oysters. The diacylglycerol kinase delta (*Dgkd*) gene was consistently hypomethylated in somatic muscle and gonadal tissue of female oysters. Additionally, genes involved in Rho protein signal transduction were found to be consistently differentially methylated in both muscle and

gonadal tissue [40]. In oyster gonads, multiple genes (e.g. *Foxl2*, *Dmrt1*, *Dgkd*), were discovered to be involved in sex differentiation, whereas these genes where not found to be differentially methylated in gill tissue in this study [28–31, 40]. Additionally, DNA methylation in gonad tissue was often found to be hypermethylated among males compared to females [29, 30, 40]. In our study, males or females did not show consistent hyper or hypomethylation for DMRs and DMGs. Although the enrichment for GO terms related to metabolism and energy homeostasis pathways do not overlap with DNA methylation patterns found for gonad tissue in other oysters, and may therefore be indicative of functional differences between tissues, a direct comparison of DNA methylation patterns between gill and gonadal tissue was not performed in this study and requires further elucidation.

In *Crassostrea virginica,* differences in sex-specific gene expression were identified between mantle and gonad transcriptomes [14]. Here, differentially expressed genes found between male and female mantle tissue were associated with cell proliferation, apoptosis, and lipid transportation. Based on their findings, the authors suggest that sex-specific gene expression in mantle tissue has a specific function that could be potentially related to environmental sensing or signalling in *C. virginica* [14]. The observed enrichment in energy homeostasis and metabolism related pathways in sex-specific DMGs identified in this study could be indicative of functional processes related to sex reversal in the gills. However, to further elucidate potential functional differences in sex-specific DNA methylation of different tissues, more elaborate methylome comparisons between various tissues are required. Additionally, GO and KEGG enrichment analysis are both largely dependent on available gene annotations, and so our discussion on the occurrence of functional sex-specific DNA methylation in the gills is limited to currently available reference genomes and gene annotations.

Causality dilemma of the role of somatic DNA methylation in sex reversal

Our findings clearly show the presence of sex-specific DNA methylation in gill tissue of *O. edulis*, however, it remains unknown where in the process of sex reversal this gill tissue DNA methylation plays a role. Sex steroids are known to not only influence sex differentiation in reproductive tissues, but can also affect cell fates in somatic tissues all throughout the body [92]. The concept of altered whole-body methylomes or transcriptomes in response to treatment with endocrine disrupting chemicals is widely observed in fish [97–99]. Interestingly, DNA methylation can also affect sex differentiation vice versa [100]. Based on this, it could be hypothesized that sex-specific DNA methylation of the gills occurs prior to gonadal sex differentiation, and plays a more active part in sex reversal. Environmental stressors like starvation have been demonstrated to affect energy homeostasis and metabolism pathways in the gills of bivalves through influencing gene expression [28, 67]. Hence, it could be inferred that environmental stressors induce changes in gill DNA methylation, where a remodeling of the energy balance could subsequently induce sex differentiation in the gonads. In this case, gill DNA methylation would represent a more active player in sex reversal. Although gill and gonadal samples were collected simultaneously in this study, we do not know whether the phenotypic sex represented by the gonads is similarly represented by the DNA methylation state of the gills. Furthermore, to better understand differences in sex-specific DNA methylation between different tissues, the effect of sex-specific DNA methylation on gene expression and corresponding functionality should be elucidated.

Non-lethal sex identification using epigenetic markers

Sex identification is extremely relevant for understanding the process and dynamics of sex reversal in sequential hermaphrodites. Currently, sex identification in oysters is complicated by the dependency on gonadal tissue, of which sampling is lethal. With the use of anesthetics, some somatic tissues can be sampled non-lethally (e.g. abductor muscle, gill, and mantle tissue). Therefore, the use of molecular markers, that rely on somatic tissues for sex identification, provide a promising non-lethal alternative. Epigenetic markers are currently applied to assess sex and age, or response to pollutants in various marine species [101–103]. In our study, comparison of gill methylomes between male and female oysters resulted in the characterization of 125 DMGs. Differential methylation on these genes could provide the basis for generating epigenetic markers that can assess the current sex phenotype of an oyster. Additionally, the distinct DNA methylation profile of hermaphrodite oysters would allow for a higher resolution of sex identification, whereby hermaphrodites could be distinguished from male or female individuals. Collectively, our findings indicate the potential of using somatic gill tissue for non-lethal sex identification utilizing epigenetic markers that can predict the current sex phenotype of an oyster.

Conclusion

In conclusion, this study is the first to characterize sex-specific DNA methylation in somatic gill tissue of a sequential hermaphrodite invertebrate. Our findings

suggest that hermaphrodite oysters display distinct differences in gill DNA methylation patterns compared to male and female individuals. Annotation of differentially methylated genes resulted in significant enrichment of pathways associated with energy homeostasis, metabolism, and innate immunity. Collectively, our data suggests that sequential hermaphrodites display an alternative state that represents the epigenetic reprogramming required for sex reversal in a somatic tissue. Additionally, the characterized differentially methylated loci and regions between sex phenotypes from somatic gill tissue provide a basis for non-lethal alternatives to sex identification with epigenetic markers. Taken together, this study contributes to the understanding of epigenetic mechanisms underlying sex reversal in different sex phenotypes of the flat oyster, and shows the relevance of studying sex-specific DNA methylation in somatic tissues in relation to sex reversal.

Materials and methods

Sampling site and collection

In this study, DNA methylomes were obtained from whole-genome sequencing of gill tissue of 35 European flat oysters (*Ostrea edulis*) of different sex phenotypes. Oysters were collected by dredging in April and September 2023, and April 2024 in Grevelingenmeer, the Netherlands (53°30′40″N, 08°06′20″ E). Individuals of similar shell length (74.1 ± 7.45 mm; Supplementary FiS1B) were selected and gill tissue was collected and preserved with RNAlater or snap-frozen using liquid nitrogen. All gill tissue samples were stored at −80 °C until further use. Oysters were collected in the context of the national monitoring for mollusc diseases in the Netherlands. Samples from gill, mantle, and digestive diverticulum tissue were tested for the presence of the haplosporidian *Bonamia ostreae,* using species-specific real time PCR as described in Kamermans et al. (2023). Two oysters (nr. 3 and 17) tested positive for an infection of *B. ostreae.* We did not correct for this in our analysis, as other physiological differences between individuals were not assessed nor included in this analysis.

Histological sex identification

Cross sections of tissue representing both reproductive, respiratory, and digestive organs were embedded in paraffin. Sections (± 5 µm) were stained with haematoxylin–eosin for histological observation. Each oyster was categorized a sex stage and gonad development index, according to the study of da Silva et al. (2009) [15]. The five sex stages are as follows: *male* (M), *female* (F), *hermaphrodite predominantly male* (HPM), *hermaphrodite predominantly female* (HPF), or *hermaphrodite both sexes equally present* (HBS). The gonad development index was considered as follows: *Inactive or resting gonad* (0), *early gametogenesis* (1), *advanced gametogenesis* (2), *mature* (3), *partially spawned gonad* (4), *reabsorbing gonad* (5). Oysters that displayed no clear gonad tissue and were therefore categorized to be in the inactive or resting gonad phase (0) were not used for analysis. In total, 35 oysters were used for DNA methylome sequencing; 9 M, 8 F, 5 HPM, 9 HPF, and 4 HBS oysters. An overview of all histological images can be found in the supplementary material (Supplementary Figure S5).

DNA extraction

Genomic DNA was extracted from oyster gill tissue using the Qiagen Gentra Kit for genomic DNA or Monarch HMW DNA extraction kit for tissue, according to the manufacturer's instructions (Qiagen catalog no. 158667; NEB catalog no. T3060). Sample input varied from 20 to 30 mg of frozen gill tissue and was grinded using liquid nitrogen. Long DNA (> 20 Kb) was sheared using g-TUBES (Covaris, USA) in 1 min centrifugation steps of 8, 10, 12, 14 (x1000G) respectively. Short reads were eliminated using the SRE XS PacBio kit, following the manufacturer's instructions (Pacific Biosciences, Menlo Park, CA, USA). DNA was quantified using the HS Qubit assay (Life Technologies, ThermoFisher Scientific). Quality and length of DNA was visualized using agarose gel electrophoresis.

Library preparation & sequencing

To prepare samples for whole-genome sequencing using the Oxford Nanopore Platform (ONT, Oxford, UK), short-read eliminated samples were used for end-prep and DNA repair, followed by barcode and adapter ligation according to the native barcoding protocol (SQK-NBD114-24). Up to a maximum of five oysters were simultaneously sequenced using PromethtION R10.4.1 flowcells (FLO-PRO114M) on a PromethION-24 device, using MinKNOW software versions: 23.04.5 (July 2023), 23.07.12 (December 2023), 24.02.19 (May 2024), and 24.06.15 (December 2024). A minimum read quality threshold of 7 was applied.

Bioinformatics

Raw read processing

Raw sequenced reads (POD5) were basecalled using Dorado v0.4.1 [104], allowing for simultaneous super accuracy basecalling (SUP) of canonical basepairs using model dna_r10.4.1_e8.2_400bps_sup@4.2.0, and 5mC modifications using the *–modified-bases 5mC* flag for the detection of modified bases. The reads were mapped to the reference genome xbOstEdul1.1 (NCBI RefSeq Assembly: GCF_947568905.1 [105]) with minimap2

[106] as a built-in tool within the Dorado *basecaller* function. After mapping, the reads were demultiplexed using the *demux* function of Dorado. Mapped BAM files were then filtered on a minimal mapping quality of 60 and all unmapped reads or secondary alignments were removed using *Samtools* v1.17 [107]. After filtering, BAM files were sorted and indexed using *Samtools.* Descriptive statistics for BAM files were generated using NanoPack2 v1.12.0 [108].

CpG calling

The *pileup* function of Modkit v0.2.1 (https://github.com/nanoporetech/modkit) was used to call CpGs from the mapped BAM files to generate BEDmethyl output files, using the xbOstEdul1.1 reference genome [105]. For some CpG sites more than half of the reads were identified as Ndel, indicating the read contains a deletion on this site compared to the reference genome. Reads where the number of Ndels was ≥60% of the total coverage for the corresponding CpG site were removed from the dataset.

Differential methylation analysis

Characterization of differentially methylated loci and regions

BEDmethyl files generated by Modkit were used as input for methylKit v.0.99.2 in R v.4.3.3 [109, 110]. Methylation percentages were calculated for every CpG site by dividing the sum of methylated CpGs by the total number of CpGs covered. Methylation calls were filtered to a minimum required coverage of 3 reads per CpG site for all individuals. Methylation call distributions between samples were normalized using the *normalizeCoverage* function to reduce the potential bias in varying coverage among individuals. For pairwise comparisons between sex phenotypes, data was reorganized to include only the individuals pertaining the selected sex phenotypes, using the *reorganize* function. CpG sites of individuals from two sex phenotypes were then merged using the *unite* function. To correct for a potential effect of maturation development stage on DNA methylation, maturation stage was added as a covariate.

Using a logistic regression, differentially methylated loci (DMLs) were identified for each pairwise comparison, using the *calculateDiffMeth* function in methylKit. *P*-values were adjusted for multiple testing using the Benjamin-Hochberg correction. DMLs were defined as loci with a minimal methylation difference of 20% between the two compared sex phenotypes, and a q-value <0.01 (BH corrected). For every pairwise comparison, the number of hypermethylated and hypomethylated DMLs were determined whereby a hypermethylated DML was defined as a CpG site where the treatment group was more methylated than the control group. A hypomethylated DML was defined as a CpG locus where the treatment group was less methylated than the control group.

Differentially methylated regions (DMRs) were identified using a sliding-window approach of 200 bp window slides and 100 bp intervals, using the *tileMethylCounts* function from methylKit, with maturation stage added as a covariate. Only windows containing ≥5 CG loci (*cov. bases*), a minimal difference in methylation percentage of 20%, and BH-adjusted q-value <0.01 were considered as DMRs. Hypermethylated DMRs were defined as DMRs where the treatment group was hypermethylated compared to the control group. Hypomethylated DMRs were defined as DMRs where the treatment group was hypomethylated compared to the control group. Differentially methylated loci and regions were visualized from BED files using IGV v2.19.1 [111].

To identify the distribution of DMRs over genomic features (promoter, exon, intron, intergenic region), the position of genomic features was extracted from the reference genome using *readTranscriptFeatures* from methylKit. Subsequently DMRs were annotated to these genomic features using *annotateWithGeneParts* function from the genomation package [112]. Promoters were defined as regions 1000 bp upstream or downstream of Transcription Start Sites (TSS). To test if there was an association between genomic location of DMRs and the genomic location of all CpGs with minimal coverage of 3 for all individuals, chi-square contingency pairwise tests were used.

Identifying differentially methylated genes

To identify the differentially methylated genes (DMGs), genes overlapping with DMRs, the DMRs within 100 bp proximity of one another were first merged together. Subsequently, gene coordinates were extracted from the reference annotation (GCF_947568905.1_xbOstEdul1.1_genomic.gtf.gz [105]) using the *gene* function of GenomicFeatures [113]. Genetic description and GeneID were added using *getGenes* from mygene [114]. Genes were considered statistically differentially methylated if they contained at least one DMR with minimal methylation percentage of 20% and BH-adjusted q-value <0.01.

To analyse functional enrichment of annotated DMGs, Gene Ontology (GO) analysis was performed using TopGO in Bioconductor [115]. Using the Gene Annotation File (GAF) the reference genome (GCF_947568905.1-RS_2023_05_gene_ontology.gaf), GO terms were annotated to geneIDs and separated based on GO term categories: Biological Processes (BP), Cellular Components (CC), or Molecular Function (MF). Go terms with $p < 0.001$ were considered significantly enriched by DMR-overlapping genes.

Heatmaps were generated using the pheatmap package in R [116]. The upset plot was generating using UpSetR [117].

Kyoto Encyclopedia of Genes and Genomes (KEGG) enrichment analysis was performed using the KEGGrest [118] package in R.Enrichment pathways were imported for *Ostrea edulis* (organism code: "oed"; RefSeq Assembly: GCF_947568905.1) using *keggLink*. Enrichment analysis was performed using the *enrichKEGG* function from the clusterProfiler package [119]. A Benjamini–Hochberg adjustment of p-values was applied to correct for False Discovery Rate (FDR).

General statistical analysis

To check for differences in average shell length and average sequenced Gb per sex phenotype, one-way ANOVAs were performed using the *stats* package from R [120]. With Shapiro–Wilk's and Levene's test, deviations from normality and homogeneity of variance of the residuals were validated using the *car* package v3.1.3 [121].

Abbreviations

M	Male
F	Female
HPM	Hermaphrodite predominantly male
HPF	Hermaphrodite predominantly female
HBS	Hermaphrodite both sexes equally present
DML	Differentially methylated loci
DMR	Differentially methylated region
DMG	Differentially methylated gene
GO	Gene Ontology
KEGG	Kyoto Encyclopedia of Genes and Genomes
FDR	False discovery rate

Supplementary Information

The online version contains supplementary material available at https://doi.org/10.1186/s12864-025-11736-1.

Supplementary Mayetrial 1: Supplementary Table S1. Overview of all 35 sequenced flat oyster individuals with information on shell length, date and location of oyster collection, DNA extraction, and sequencing results.

Supplementary Material 2: Supplementary Table S2. Overview of the number of DMLs identified from all pairwise comparisons between the five sex phenotypes (M, F, HPM, HPF, and HBS). DMLs are defined as CpGs with a minimal difference in average methylation percentage of 20% between compared groups, and BH-adjusted q-value<0.01.

Supplementary Material 3: Supplementary Table S3. Pearson's Chi-squared pairwise comparisons between proportions of genomic locations of significant DMLs compared with all CpGs with 3x coverage detected between all 5 sex phenotypes.

Supplementary Material 4: Supplementary Table S4. Overview of the number of differentially methylated regions (DMRs) identified from all pairwise comparisons between the five sex phenotypes (M, F, HPM, HPF, and HBS). DMRs are defined as regions of at least 200bp, containing ≥5 CpG loci, with a minimal difference in average methylation percentage of 20% between compared groups, and BH-adjusted q-value<0.01.

Supplementary Material 5: Supplementary Table S5. Overview of the top 10 hypermethylated and hypomethylated DMGs for each pairwise comparison between all five sex phenotypes (M, F, HPM, HPF, HBS).

Supplementary Material 6: Supplementary Table S6. Overview of uniquely identified DMGs between true male and female oyster individuals.

Supplementary Material 7: Supplementary Figure S1. A) Boxplot of shell length of flat oyster individuals per sex phenotype. B) Boxplot of total number of sequenced base pairs (Gb) per flat oyster individual for each sex phenotype.

Supplementary Material 8: Supplementary Figure S2. Differential methylation characterized for each pairwise comparison between the five sex phenotypes. A). Number and genomic distribution of DMLs identified for each pairwise comparison. B) Number and genomic distribution of DMRs identified between each pairwise comparison.

Supplementary Material 9: Supplementary Figure S3. Heatmap of Gene Ontology (GO) annotation of DMGs (n=2,576) significantly enriched for 45 Cellular Components (p<0.001). CC were clustered hierarchically with Pearson's correlation coefficient. The colour scale represents log10(p-values) of Fisher's exact test.

Supplementary Material 10: Supplementary Figure S4. Heatmap of Gene Ontology (GO) annotation of DMGs (n=2,576) significantly enriched for 64 Molecular Functions (p<0.001). MF were clustered hierarchically with Pearson's correlation coefficient. The colour scale represents log10(p-values) of Fisher's exact test.

Supplementary Material 11: Supplementary Figure S5. Micrographs of histological sections of *Ostrea edulis* individuals showing the gonad area.

Acknowledgements

We would like to thank Betty van Gelderen and Michal Voorbergen-Laarman from Wageningen Bioveterinary Research for their major support in sample collection. We extend our gratitude to Nicky Brouwer for her support in sample collection and lab work during the initial stages of this study. We also thank Bert Dibbits and Kimberley Laport for sharing their insights and suggestions in the lab. Samples used in this study were collected in addition to oysters collected in the context of the national monitoring for mollusc diseases in the Netherlands (project no/WOT-01-002-032). We thank the crew of the vessel Regulus for their support in oyster collection.

Author's contributions

SV, HJM, and RN conceptualized the study. SV carried out the methodology and sequencing. Data analysis was performed by SV and HJM. Writing of the manuscript was done by SV, and review & editing of the manuscript was carried out by SV, ME, HJM, PK, AM, and RN. RN was involved in supervision of the research. SV and PK acquired funding.

Funding

Whole genome sequencing was made possible with financial support of the Centre of Genetic Resources (CGN) of Wageningen University and Research (project no/WOT-03–001-069).

Data availability

All processed sequencing data generated in this study (BAM format) have been submitted to the European Nucleotide Archive (ENA; https://www.ebi.ac.uk/ena/) under project number PRJEB85091 with accession number ERP168521.

Declarations

Ethics approval and consent to participate

Not applicable.

Consent for publication

Not applicable.

Competing interests

The authors declare no competing interests.

Received: 28 February 2025 Accepted: 21 May 2025
Published online: 06 June 2025

References

1. Jones PA. Functions of DNA methylation: islands, start sites, gene bodies and beyond. Nat Rev Genet. 2012;13(7):484–92.
2. Cheng T, Wang Y, Huang J, Chen X, Zhao X, Gao S, et al. Our recent progress in epigenetic research using the model ciliate. Tetrahymena thermophila Mar Life Sci Technol. 2019;1(1):4–14.
3. Okano M, Bell DW, Haber DA, Li E. DNA Methyltransferases Dnmt3a and Dnmt3b Are Essential for De Novo Methylation and Mammalian Development. Cell. 1999;99(3):247–57.
4. Sheldon EL, Schrey AW, Lauer ME, Martin LB. Epigenetic potential: Promoter CpG content positively covaries with lifespan and is dependent on gene function among vertebrates. J Hered. 2023;114(3):207–18.
5. Klughammer J, Romanovskaia D, Nemc A, Posautz A, Seid CA, Schuster LC, et al. Comparative analysis of genome-scale, base-resolution DNA methylation profiles across 580 animal species. Nat Commun. 2023;14(1):232.
6. Sarda S, Zeng J, Hunt BG, Yi SV. The Evolution of Invertebrate Gene Body Methylation. Mol Biol Evol. 2012;29(8):1907–16.
7. Suzuki MM, Kerr ARW, De Sousa D, Bird A. CpG methylation is targeted to transcription units in an invertebrate genome. Genome Res. 2007;17(5):625–31.
8. Roberts SB, Gavery MR. Is There a Relationship between DNA Methylation and Phenotypic Plasticity in Invertebrates? Front Physiol . 2012;2. Available from: http://journal.frontiersin.org/article/10.3389/fphys.2011.00116/abstract. Cited 2024 May 22.
9. Zhang H, Tan K, Li S, Ma H, Zheng H. DNA methylation in molluscs growth and development: An overview. Aquac Res. 2022;53(14):4893–900.
10. Whiteley SL, Castelli MA, Dissanayake DSB, Holleley CE, Georges A. Temperature-Induced Sex Reversal in Reptiles: Prevalence, Discovery, and Evolutionary Implications. Sex Dev. 2021;15(1–3):148–56.
11. Akashi H, Hasui D, Ueda K, Ishikawa M, Takeda M, Miyagawa S. Understanding the role of environmental temperature on sex determination through comparative studies in reptiles and amphibians. J Exp Zool Part Ecol Integr Physiol. 2024;341(1):48–59.
12. Casas L, Saborido-Rey F. Environmental Cues and Mechanisms Underpinning Sex Change in Fish. Sex Dev. 2021;15(1–3):108–21.
13. Adzigbli L, Wang Z, Lai Z, Li J, Deng Y. Sex determination in pearl oyster: A mini review. Aquac Rep. 2019;15: 100214.
14. Proestou DA, Delomas TA, Sullivan ME, Markey LK. Sex-specific gene expression in eastern oyster, Crassostrea virginica, gonad and mantle tissues. Invertebr Biol. 2024;143(1):e12418.
15. Da Silva PM, Fuentes J, Villalba A. Differences in gametogenic cycle among strains of the European flat oyster Ostrea edulis and relationship between gametogenesis and bonamiosis. Aquaculture. 2009;287(3–4):253–65.
16. Guerrero-Tortolero DA, Campos-Ramos R. Sex Reversal and Determination and Sex Control in Shrimp and Prawn. In: Wang H, Piferrer F, Chen S, Shen Z, editors. Sex Control in Aquaculture . 1st ed. Wiley; 2018. p. 705–22. Available from: https://onlinelibrary.wiley.com/doi/10.1002/9781119127291.ch36. Cited 2024 Sep 13.
17. Compton A, Tu Z. Natural and Engineered Sex Ratio Distortion in Insects. Front Ecol Evol. 2022;10: 884159.
18. De Lisle SP, Bolnick DI. Male and female reproductive fitness costs of an immune response in natural populations*. Evolution. 2021;75(10):2509–23.
19. Arendt JD, Reznick DN, López-Sepulcre A. Replicated Origin Of Female-Biased Adult Sex Ratio In Introduced Populations Of The Trinidadian Guppy (*Poecilia Reticulata*): Adult Sex Ratio In Guppies. Evolution. 2014;n/a-n/a.
20. Senior AM, Lim JN, Nakagawa S. The fitness consequences of environmental sex reversal in fish: a quantitative review. Biol Rev. 2012;87(4):900–11.
21. Yamaguchi S, Iwasa Y. Advantage for the sex changer who retains the gonad of the nonfunctional sex. Behav Ecol Sociobiol. 2017;71(2):39.
22. Shao C, Li Q, Chen S, Zhang P, Lian J, Hu Q, et al. Epigenetic modification and inheritance in sexual reversal of fish. Genome Res. 2014;24(4):604–15.
23. Todd EV, Ortega-Recalde O, Liu H, Lamm MS, Rutherford KM, Cross H, et al. Stress, novel sex genes, and epigenetic reprogramming orchestrate socially controlled sex change. Sci Adv. 2019;5(7):eaaw7006.
24. Liu Z, Zhou T, Gao D. Genetic and epigenetic regulation of growth, reproduction, disease resistance and stress responses in aquaculture. Front Genet. 2022;13:994471.
25. Davenel A, González R, Suquet M, Quellec S, Robert R. Individual monitoring of gonad development in the European flat oyster Ostrea edulis by in vivo magnetic resonance imaging. Aquaculture. 2010;307(1–2):165–9.
26. Lee HJ, Lee HM, Hong HK, Hur YB, Choi KS. The Annual Reproductive Cycle and Reproductive Effort of the Pacific Oyster Crassostrea gigas from a Tidal Flat in Incheon Bay on the West Coast of Korea. Ocean Sci J. 2024;59(1):2.
27. Venkataraman YR, White SJ, Roberts SB. Differential DNA methylation in Pacific oyster reproductive tissue in response to ocean acidification. BMC Genomics. 2022;23(1):556.
28. Sun D, Yu H, Li Q. Starvation-induced changes in sex ratio involve alterations in sex-related gene expression and methylation in Pacific oyster Crassostrea gigas. Comp Biochem Physiol B Biochem Mol Biol. 2023;267: 110863.
29. Sun D, Li Q, Yu H. DNA methylation differences between male and female gonads of the oyster reveal the role of epigenetics in sex determination. Gene. 2022;820:146260.
30. Sun D, Yu H, Kong L, Liu S, Xu C, Li Q. The role of DNA methylation reprogramming during sex determination and sex reversal in the Pacific oyster Crassostrea gigas. Int J Biol Macromol. 2024;259:128964.
31. Broquard C, Saowaros SA, Lepoittevin M, Degremont L, Lamy JB, Morga B, et al. Gonadal transcriptomes associated with sex phenotypes provide potential male and female candidate genes of sex determination or early differentiation in Crassostrea gigas, a sequential hermaphrodite mollusc. BMC Genomics. 2021;22(1):609.
32. Joyce A, Holthuis TD, Charrier G, Lindegarth S. Experimental Effects of Temperature and Photoperiod on Synchrony of Gametogenesis and Sex Ratio in the European Oyster *Ostrea edulis* (*Linnaeus*). J Shellfish Res. 2013;32(2):447–58.
33. Zhang X, Li Q, Kong L, Yu H. DNA methylation frequency and epigenetic variability of the Pacific oyster Crassostrea gigas in relation to the gametogenesis. Fish Sci. 2018;84(5):789–97.
34. Yue C, Li Q, Yu H. Gonad Transcriptome Analysis of the Pacific Oyster Crassostrea gigas Identifies Potential Genes Regulating the Sex Determination and Differentiation Process. Mar Biotechnol. 2018;20(2):206–19.
35. Diaz-Almela E, Boudry P, Launey S, Bonhomme F, Lapègue S. Reduced Female Gene Flow in the European Flat Oyster Ostrea edulis. J Hered. 2004;95(6):510–6.
36. Broquard C, Martinez AS, Maurouard E, Lamy JB, Dégremont L. Sex determination in the oyster Crassostrea gigas - A large longitudinal study of population sex ratios and individual sex changes. Aquaculture. 2020;515:734555.
37. Feng M, Tan K, Zhang H, Zheng H. Factors affecting sex reversal in bivalves: Case study on the effects of sex reversal on growth of offspring employing the noble scallop Chlamys nobilis. Aquaculture. 2023;566:739192.
38. Nicolini F, Ghiselli F, Luchetti A, Milani L. Bivalves as Emerging Model Systems to Study the Mechanisms and Evolution of Sex Determination: A Genomic Point of View. Genome Biol Evol. 2023;15(10):evad181.
39. Kvist J, Athanàsio CG, Pfrender ME, Brown JB, Colbourne JK, Mirbahai L. A comprehensive epigenomic analysis of phenotypically distinguishable, genetically identical female and male Daphnia pulex. BMC Genomics. 2020;21(1):17.
40. Teng W, Xu C, Liu S, Yu H, Kong L, Li Q. DNA Methylation of Somatic Tissues in Oysters is Influenced by Sex and Heredity. Mar Biotechnol. 2025;27(1):31.
41. Engelsma M, Kerkhoff S, Roozenburg I, Haenen O, Van Gool A, Sistermans W, et al. Epidemiology of Bonamia ostreae infecting European flat oysters Ostrea edulis from Lake Grevelingen. The Netherlands Mar Ecol Prog Ser. 2010;409:131–42.
42. Kamermans P, Blanco A, Van Dalen P, Engelsma M, Bakker N, Jacobs P, et al. *Bonamia* -free flat oyster (*Ostrea edulis* L.) seed for restoration projects: non-destructive screening of broodstock, hatchery production and test for *Bonamia* -tolerance. Aquat Living Resour. 2023;36:11.
43. Coen L, Brumbaugh R, Bushek D, Grizzle R, Luckenbach M, Posey M, et al. Ecosystem services related to oyster restoration. Mar Ecol Prog Ser. 2007;341:303–7.

44. Potet M, Fabien A, Chaudemanche S, Sebaibi N, Guillet T, Gachelin S, et al. Which concrete substrate suits you? Ostrea edulis larval preferences and implications for shellfish restoration in Europe. Ecol Eng. 2021;162:106159.
45. Smyth D, Roberts D. The European oyster (Ostrea edulis) and its epibiotic succession. Hydrobiologia. 2010;655(1):25–36.
46. van Banning P. Haplosporidian diseases of imported oysters, Ostrea edulis, in Dutch estuaries. Mar Fish Rev. 1979;41(1–2):8.
47. Helmer L, Farrell P, Hendy I, Harding S, Robertson M, Preston J. Active management is required to turn the tide for depleted *Ostrea edulis* stocks from the effects of overfishing, disease and invasive species. PeerJ. 2019;7:e6431.
48. OSPAR BDC, 2020. Status Assessment 2020 - European flat oyster and Ostrea edulis beds. Available at: https://oap.ospar.org/en/ospar-assessments/committee-assessments/biodiversity-committee/status-assessments/european-flat-oyster/.
49. OSPAR Commission. Invertebrates. Available from: https://www.ospar.org/work-areas/bdc/species-habitats/list-of-threatened-declining-species-habitats/invertebrates. Cited 2025 Jan 25.
50. Colsoul B, Pouvreau S, Di Poi C, Pouil S, Merk V, Peter C, et al. Addressing critical limitations of oyster (*Ostrea edulis*) restoration: Identification of nature-based substrates for hatchery production and recruitment in the field. Aquat Conserv Mar Freshw Ecosyst. 2020;30(11):2101–15.
51. Bos OG, Duarte-Pedrosa S, Didderen K, Bergsma JH, Heye S, Kamermans P. Performance of European oysters (Ostrea edulis L.) in the Dutch North Sea, across five restoration pilots. Front Mar Sci. 2023;10:1233744.
52. Kamphausen L, Jensen A, Hawkins L. Unusually High Proportion of Males in a Collapsing Population of Commercially Fished Oysters (*Ostrea edulis*) in the Solent. United Kingdom J Shellfish Res. 2011;30(2):217–22.
53. Jiang S, Qiu L, Wang L, Jia Z, Lv Z, Wang M, et al. Transcriptomic and Quantitative Proteomic Analyses Provide Insights Into the Phagocytic Killing of Hemocytes in the Oyster Crassostrea gigas. Front Immunol. 2018;9:1280.
54. Venney CJ, Anastasiadi D, Wellenreuther M, Bernatchez L. The Evolutionary Complexities of DNA Methylation in Animals: From Plasticity to Genetic Evolution. Genome Biol Evol. 2023;15(12):evad216.
55. Wang F, Gao T, Yang X, Wu Q, Li Y, Ye M, et al. DNA methylation plays a critical role in testicular maintenance, but not in sex determination of male tilapia Oreochromis niloticus. Aquaculture. 2024;595:741455.
56. Collin R. Phylogenetic Patterns and Phenotypic Plasticity of Molluscan Sexual Systems. Integr Comp Biol. 2013;53(4):723–35.
57. Piferrer F. Epigenetic mechanisms in sex determination and in the evolutionary transitions between sexual systems. Philos Trans R Soc B Biol Sci. 1832;2021(376):20200110.
58. Gombeau K, Pereira S, Ravanat JL, Camilleri V, Cavalie I, Bourdineaud JP, et al. Depleted uranium induces sex- and tissue-specific methylation patterns in adult zebrafish. J Environ Radioact. 2016;154:25–33.
59. Bock SL, Smaga CR, McCoy JA, Parrott BB. Genome-wide DNA methylation patterns harbour signatures of hatchling sex and past incubation temperature in a species with environmental sex determination. Mol Ecol. 2022;31(21):5487–505.
60. Zhuang QKW, Galvez JH, Xiao Q, AlOgayil N, Hyacinthe J, Taketo T, et al. Sex Chromosomes and Sex Phenotype Contribute to Biased DNA Methylation in Mouse Liver. Cells. 2020;9(6):1436.
61. Glastad KM, Gokhale K, Liebig J, Goodisman MAD. The caste- and sex-specific DNA methylome of the termite Zootermopsis nevadensis. Sci Rep. 2016;6(1):37110.
62. Domingos JA, Budd AM, Banh QQ, Goldsbury JA, Zenger KR, Jerry DR. Sex-specific dmrt1 and cyp19a1 methylation and alternative splicing in gonads of the protandrous hermaphrodite barramundi. PLOS ONE. 2018;13(9):e0204182.
63. Gavery MR, Roberts SB. Predominant intragenic methylation is associated with gene expression characteristics in a bivalve mollusc. PeerJ. 2013;1:e215.
64. Johnson KM, Kelly MW. Population epigenetic divergence exceeds genetic divergence in the Eastern oyster *Crassostrea virginica* in the Northern Gulf of Mexico. Evol Appl. 2020;13(5):945–59.
65. Johnson KM, Sirovy KA, Kelly MW. Differential DNA methylation across environments has no effect on gene expression in the eastern oyster. J Anim Ecol. 2022;91(6):1135–47.
66. Li Y, Teng W, Xu C, Yu H, Kong L, Liu S, et al. Intergenerational transfer and sex differences of DNA methylation patterns in the Pacific oyster (*Crassostrea gigas*) . 2022. Available from: http://biorxiv.org/lookup/doi/10.1101/2022.02.22.481396. Cited 2024 May 10.
67. Wang X, Wei Y, Cong R, Wang W, Qi H, Zhang G, et al. DNA methylation-mediated energy metabolism provides new insight into the quality losses during oyster reproductive process. Aquaculture. 2024;583: 740595.
68. Liang ZW, Li SY, Zhang XL, Chen CY, Sun WJ, Gu ZQ, et al. Morphological change and differential proteomics analysis of gill in Mytilus coruscus under starvation. Front Physiol. 2023;14:1150521.
69. Tan Y, Li Y, Ren L, Fu H, Li Q, Liu S. Integrative proteome and metabolome analyses reveal molecular basis underlying growth and nutrient composition in the Pacific oyster. Crassostrea gigas J Proteomics. 2024;290:105021.
70. Tu-Sekine B, Kim SF. The Inositol Phosphate System—A Coordinator of Metabolic Adaptability. Int J Mol Sci. 2022;23(12):6747.
71. Hassan MM, Qin JG, Li X. Gametogenesis, sex ratio and energy metabolism in Ostrea angasi: implications for the reproductive strategy of spermcasting marine bivalves. J Molluscan Stud. 2018;84(1):38–45.
72. Frolov AV, Pankov SL. The reproduction strategy of oyster ostrea edulis L. from the biochemical point of view. Comp Biochem Physiol Part B Comp Biochem. 1992;103(1):161–82.
73. Fang Y, Yang X, Zhang S, Chen X, Lin G, Zhang Y, et al. Transcriptome study on immune response against Vibrio parahaemolyticus challenge in gill of abalone Haliotis discus hannai Ino. Front Mar Sci. 2022;9:956317.
74. Dong L, Sun Y, Chu M, Xie Y, Wang P, Li B, et al. Exploration of Response Mechanisms in the Gills of Pacific Oyster (Crassostrea gigas) to Cadmium Exposure through Integrative Metabolomic and Transcriptomic Analyses. Animals. 2024;14(16):2318.
75. Li M, Wang Y, Tang Z, Wang H, Hu J, Bao Z, et al. Expression Plasticity of Peroxisomal Acyl-Coenzyme A Oxidase Genes Implies Their Involvement in Redox Regulation in Scallops Exposed to PST-Producing Alexandrium. Mar Drugs. 2022;20(8):472.
76. Zhang Z, Li X, Vandepeer M, Zhao W. Effects of water temperature and air exposure on the lysosomal membrane stability of hemocytes in pacific oysters, Crassostrea gigas (Thunberg). Aquaculture. 2006;256(1–4):502–9.
77. Brokordt K, Defranchi Y, Espósito I, Cárcamo C, Schmitt P, Mercado L, et al. Reproduction Immunity Trade-Off in a Mollusk: Hemocyte Energy Metabolism Underlies Cellular and Molecular Immune Responses. Front Physiol. 2019;10:77.
78. Huvet A, Normand J, Fleury E, Quillien V, Fabioux C, Boudry P. Reproductive effort of Pacific oysters: A trait associated with susceptibility to summer mortality. Aquaculture. 2010;304(1–4):95–9.
79. Delaporte M, Soudant P, Lambert C, Moal J, Pouvreau S, Samain JF. Impact of food availability on energy storage and defense related hemocyte parameters of the Pacific oyster Crassostrea gigas during an experimental reproductive cycle. Aquaculture. 2006;254(1–4):571–82.
80. Li Y, Qin JG, Li X, Benkendorff K. Assessment of metabolic and immune changes in postspawning Pacific oyster Crassostrea gigas: identification of a critical period of vulnerability after spawning: A critical period of vulnerability in postspawning C. gigas. Aquac Res. 2010;41(9):e155-65.
81. Trotman JB, Giltmier AJ, Mukherjee C, Schoenberg DR. RNA guanine-7 methyltransferase catalyzes the methylation of cytoplasmically recapped RNAs. Nucleic Acids Res. 2017;45(18):10726–39.
82. Fabbri E, Capuzzo A. Cyclic AMP signaling in bivalve molluscs: an overview. J Exp Zool Part Ecol Genet Physiol. 2010;313A(4):179–200.
83. Guo X, He Y, Zhang L, Lelong C, Jouaux A. Immune and stress responses in oysters with insights on adaptation. Fish Shellfish Immunol. 2015;46(1):107–19.
84. Garcia BF, Mastrochirico-Filho VA, Gallardo-Hidalgo J, Campos-Montes GR, Medrano-Mendoza T, Rivero-Martínez PV, et al. A high-density linkage map and sex-determination loci in Pacific white shrimp (Litopenaeus vannamei). BMC Genomics. 2024;25(1):565.
85. Fan YJ, Gittis AH, Juge F, Qiu C, Xu YZ, Rabinow L. Multifunctional RNA Processing Protein SRm160 Induces Apoptosis and Regulates Eye and Genital Development in *Drosophila*. Genetics. 2014;197(4):1251–65.
86. Qiu C, Zhang Y, Fan YJ, Pang TL, Su Y, Zhan S, et al. HITS-CLIP reveals sex-differential RNA binding and alterative splicing regulation of SRm160 in Drosophila. J Mol Cell Biol. 2019;11(2):170–81.

87. Mederos SL, Duarte RC, Mastoras M, Dennis MY, Settles ML, Lau AR, et al. Effects of pairing on color change and central gene expression in lined seahorses. Genes Brain Behav. 2022;21(5):e12812.
88. Valles S, Hernández-Sánchez J, Dipp VR, Huerta-González D, Olivares-Bañuelos TN, González-Fraga J, et al. Exposure to low doses of inorganic arsenic induces transgenerational changes on behavioral and epigenetic markers in zebrafish (Danio rerio). Toxicol Appl Pharmacol. 2020;396:115002.
89. Muhetaer M, Yang M, Xia R, Lai Y, Wu J. Gender difference in arsenic biotransformation is an important metabolic basis for arsenic toxicity. BMC Pharmacol Toxicol. 2022;23(1):15.
90. Liu M, Ni H, Rong Z, Wang Z, Yan S, Liao X, et al. Gonad transcriptome analysis reveals the differences in gene expression related to sex-biased and reproduction of clam Cyclina sinensis. Front Mar Sci. 2023;9:1110587.
91. Messina A, Giacobini P. Semaphorin Signaling in the Development and Function of the Gonadotropin Hormone-Releasing Hormone System. Front Endocrinol . 2013;4. Available from: http://journal.frontiersin.org/article/10.3389/fendo.2013.00133/abstract. Cited 2025 Feb 23.
92. Zhou L, Liu F, Chen J, Yang R, Li J, Wang Z, et al. Comparative transcriptome analysis reveals sex bias in expression patterns of genes related to sex steroids and immunity in the skin of spinyhead croaker *Collichthys lucidus*. J Fish Biol. 2023;103(1):4–12.
93. Wan ZY, Xia JH, Lin G, Wang L, Lin VCL, Yue GH. Genome-wide methylation analysis identified sexually dimorphic methylated regions in hybrid tilapia. Sci Rep. 2016;6(1):35903.
94. Laing LV, Viana J, Dempster EL, Uren Webster TM, Van Aerle R, Mill J, et al. Sex-specific transcription and DNA methylation profiles of reproductive and epigenetic associated genes in the gonads and livers of breeding zebrafish. Comp Biochem Physiol A Mol Integr Physiol. 2018;222:16–25.
95. Legault LM, Breton-Larrivée M, Langford-Avelar A, Lemieux A, McGraw S. Sex-based disparities in DNA methylation and gene expression in late-gestation mouse placentas. Biol Sex Differ. 2024;15(1):2.
96. Yuan C, Mao J, Sun H, Wang Y, Guo M, Wang X, et al. Genome-wide DNA methylation profile changes associated with shell colouration in the Yesso scallop (Patinopecten yessoensis) as measured by whole-genome bisulfite sequencing. BMC Genomics. 2021;22(1):740.
97. Langston WJ. Endocrine disruption and altered sexual development in aquatic organisms: an invertebrate perspective. J Mar Biol Assoc U K. 2020;100(4):495–515.
98. Liu H, Lamm MS, Rutherford K, Black MA, Godwin JR, Gemmell NJ. Large-scale transcriptome sequencing reveals novel expression patterns for key sex-related genes in a sex-changing fish. Biol Sex Differ. 2015;6(1):26.
99. Zheng W, Xu H, Lam SH, Luo H, Karuturi RKM, Gong Z. Transcriptomic Analyses of Sexual Dimorphism of the Zebrafish Liver and the Effect of Sex Hormones. PLoS ONE. 2013;8(1):e53562.
100. Ribas L, Vanezis K, Imués MA, Piferrer F. Treatment with a DNA methyltransferase inhibitor feminizes zebrafish and induces long-term expression changes in the gonads. Epigenetics Chromatin. 2017;10(1):59.
101. Valdivieso A, Anastasiadi D, Ribas L, Piferrer F. Development of epigenetic biomarkers for the identification of sex and thermal stress in fish using DNA methylation analysis and machine learning procedures. Mol Ecol Resour. 2023;23(2):453–70.
102. Anastasiadi D, Piferrer F. A clockwork fish: Age prediction using DNA methylation-based biomarkers in the European seabass. Mol Ecol Resour. 2020;20(2):387–97.
103. Suarez-Ulloa V, Gonzalez-Romero R, Eirin-Lopez JM. Environmental epigenetics: A promising venue for developing next-generation pollution biomonitoring tools in marine invertebrates. Mar Pollut Bull. 2015;98(1–2):5–13.
104. nanoporetech/dorado . Oxford Nanopore Technologies; 2025. Available from: https://github.com/nanoporetech/dorado. Cited 2025 Feb 28.
105. Adkins P, Mrowicki R, Marine Biological Association Genome Acquisition Lab, Darwin Tree of Life Barcoding collective, Wellcome Sanger Institute Tree of Life programme, Wellcome Sanger Institute Scientific Operations: DNA Pipelines collective, et al. The genome sequence of the European flat oyster, Ostrea edulis (Linnaeus, 1758). Wellcome Open Res. 2023;8:556.
106. Li H. New strategies to improve minimap2 alignment accuracy. Bioinformatics. 2021;37(23):4572–4.
107. Danecek P, Bonfield JK, Liddle J, Marshall J, Ohan V, Pollard MO, et al. Twelve years of SAMtools and BCFtools. GigaScience. 2021;10(2):giab008.
108. De Coster W, Rademakers R. NanoPack2: population-scale evaluation of long-read sequencing data. Bioinformatics. 2023;39(5):btad311.
109. Akalin A, Kormaksson M, Li S, Garrett-Bakelman FE, Figueroa ME, Melnick A, et al. methylKit: a comprehensive R package for the analysis of genome-wide DNA methylation profiles. Genome Biol. 2012;13(10):R87.
110. R Core Team. R: A Language and Environment for Statistical Computing . Vienna, Austria: R Foundation for Statistical Computing; 2023. Available from: https://www.R-project.org/.
111. Thorvaldsdottir H, Robinson JT, Mesirov JP. Integrative Genomics Viewer (IGV): high-performance genomics data visualization and exploration. Brief Bioinform. 2013;14(2):178–92.
112. Akalin A, Franke V, Vlahoviček K, Mason CE, Schübeler D. genomation: a toolkit to summarize, annotate and visualize genomic intervals. Bioinformatics. 2015;31(7):1127–9.
113. Lawrence M, Huber W, Pagès H, Aboyoun P, Carlson M, Gentleman R, et al. Software for Computing and Annotating Genomic Ranges. PLoS Comput Biol. 2013;9(8):e1003118.
114. Adam Mark RT. mygene . Bioconductor; 2017. Available from: https://bioconductor.org/packages/mygene. Cited 2025 Jan 20.
115. Adrian Alexa JR. topGO . Bioconductor; 2017. Available from: https://bioconductor.org/packages/topGO. Cited 2025 Jan 20.
116. Kolde R. pheatmap: Pretty Heatmaps. 2018. Available from: https://github.com/raivokolde/pheatmap.
117. Conway JR, Lex A, Gehlenborg N. UpSetR: an R package for the visualization of intersecting sets and their properties. Bioinformatics. 2017;33(18):2938–40.
118. Tenenbaum D. KEGGREST . Bioconductor; 2017. Available from: https://bioconductor.org/packages/KEGGREST. Cited 2025 Jan 20.
119. Yu G, Wang LG, Han Y, He QY. clusterProfiler: an R Package for Comparing Biological Themes Among Gene Clusters. OMICS J Integr Biol. 2012;16(5):284–7.
120. R: The R Stats Package . [cited 2025 Feb 28]. Available from: https://stat.ethz.ch/R-manual/R-devel/library/stats/html/stats-package.html.
121. Fox J, Weisberg S, Price B. car: Companion to Applied Regression. 2001. p. 3.1–3. Available from: https://CRAN.R-project.org/package=car. Cited 2025 Jan 28.

Publisher's Note